

Drying Stress Development Patterns in Restrained Wood

C. N. Lazarescu *Dept. of Wood Science, Faculty of Forestry, University of British Columbia, 2424 Main Mall, Vancouver, BC, Canada, V6T 1Z4*

S. Avramidis *Dept. of Wood Science, Faculty of Forestry, University of British Columbia, 2424 Main Mall, Vancouver, BC, Canada V6T 1Z4*

ABSTRACT

The objective of this study was to investigate the restrained shrinkage effect perpendicular to grain of western hemlock during drying. Different mechanical restraint schemes were designed by using weights for partly- and a load cell for totally-restrained specimens. The drying rate was determined on free specimens, having similar wood structure, by weighting at different periods of time. The tests were performed on small clear wood specimens sawn from the tree trunk in such a manner that either the tangential or the radial direction was parallel to their length. Stress parameters were determined using resistive transducers. For each particular experimental run, green free and loaded samples were tested simultaneously while drying at 40, 60 and 80°C, and 15, 10 and 5% target moisture content. Analysis of the data points towards a strong relationship between temperature, restraining level and target moisture content.

INTRODUCTION

Optimum drying processes entail short drying times, high product quality and reasonable costs. Due to the peculiarities of wood as a colloidal-capillary-porous, non-homogeneous and anisotropic material, as well as due to the numerous interactions that take place within the wood-moisture-heat-environment system, drying is considered one of the most complex wood-processing operations. The central concern is represented by drying stresses resulted as a consequence of an uneven distribution of moisture inside the material. Excessive drying stresses will result in warped wood pieces after a drying cycle. The level of these deformations will be a strong function of the elastic parameters of the material as well as the severity of the internal moisture gradients (Armstrong and Kingston 1962, Svensson 1995).

The development and effect of wood stresses are governed by the difference of moisture content between two adjoining parts of the same material after one of them drops below the fiber saturation point. Most of the water transport in a piece of lumber takes place along the cross section and that is why several studies perpendicularly to wood grain have been carried out in the past years. A comprehensive study with Scots pine wood in tension perpendicular to the grain was done by Svensson (1997) and restrained rings by Ranta-Maunus

(1992), and by Hisada (1986) on hardwood species. The difficulty encountered by these authors is represented by creep and mechano-sorptive compliances correlated with climate change and different restraining scenarios.

The restraining capacity of a lumber core can range from total 0 to 100% depending of the severity of the drying schedule. A reasonable assumption would be that the restraining action of the higher moisture content layers is not efficient enough to totally constrain the shrinkage. Majka (2004) carried out a series of experiments, with three efficiency levels of restraining the desorption shrinkage: high, medium and low. The varied efficiency of shrinkage restraint was obtained by means of using dynamometers of different characteristics. An assumption was made that, with varied efficiency of shrinkage restraint and various process parameters, the intense drying is accompanied by high efficiency of shrinkage restraint and the mild drying is accompanied by low efficiency of shrinkage restraint.

Long drying times correlated with the strong tendency of wood to creep, particularly across the grain, lead to a lower shrinkage strain (set) in the outer layers. Often the tensile stresses, which occur during the early

drying steps, may cause checks or small cracks (Svensson 1997, Wu 1993). This is an undesirable feature especially when clear finish painting is applied to wood.

The objective of this study is to investigate the restrained shrinkage effect perpendicular to grain of western hemlock during drying. Drying tests on specimens subjected to different restraining levels will be compared with free-to-restrain specimens having similar wood structure. The experimental work will lead to a model used to quantify the drying stresses based on the developed set.

MATERIALS AND METHODS

Sampling method

Experimental equipment and the variability of the material play an important role in drying stress modeling. The interdependencies between the factors are clearly identified if the same wood structure is subjected to the same drying conditions, but different restraints. This way the factor effects can be statistically evaluated taking into account wood quality information for each sample (Pearson 2005).

Wood samples were taken from a single 80-year old western hemlock (*Tsuga heterophylla*) stem, grown in a second-growth plantation and having a diameter at breast high of 700mm.

The stem was sectioned in four 1-m-long logs, the first two being used for small 185x30x6mm³ test specimens and the other two for full-size 320x100x50 mm³ specimens. The logs were live sawn in boards having a thickness of 60mm and a width of 185mm (Fig.1). The numbering procedure of the boards included log number, structural direction (tangential or radial), wood density information (mature or juvenile) and geographic location (N, S, E or W). The boards were wrapped in plastic bags and stored in a cold room at -10°C in order to prevent water loss and decay. The final dimensions of the specimens for this part of the experiment were 185x30x6mm³ with 16x6mm² in the test region (Fig. 2).

Specimen matching was done by using a matrix numbering procedure where the rows represented wood strips having similar structure. The target moisture content was kept constant for each row temperature being the only variable:

$$S_{1TMN} = \begin{array}{c} 15\% \\ 10\% \\ 5\% \end{array} \begin{array}{|c|c|c|} \hline \overbrace{S_{1,1} \dots S_{1,5}}^{40C} & \overbrace{S_{1,6} \dots S_{1,11}}^{60C} & \overbrace{S_{1,12} \dots S_{1,17}}^{80C} \\ \hline \overbrace{S_{2,1} \dots S_{2,5}} & \overbrace{S_{2,6} \dots S_{2,11}} & \overbrace{S_{2,12} \dots S_{2,17}} \\ \hline \overbrace{S_{3,1} \dots S_{3,5}} & \overbrace{S_{3,6} \dots S_{3,11}} & \overbrace{S_{3,12} \dots S_{3,17}} \\ \hline \end{array} \quad (1)$$

where S_{ij} represent the wood specimens.

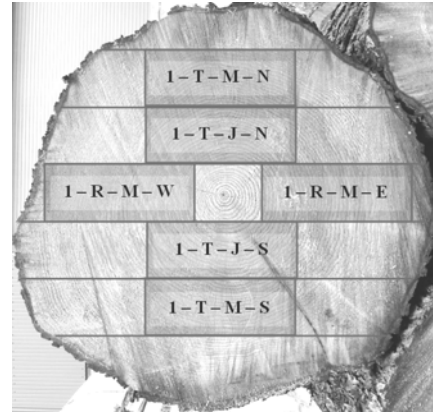


FIGURE 1. Cutting and numbering procedure for the first log: T - tangential, R - radial, M - mature, J - juvenile, N - North, S - South, E - East, W - West

The specimens were sawn from the tree trunk in such a manner that either the tangential or the radial direction was parallel to the length of the specimen. Fibre disturbances, knots and compression wood were avoided. The small size of the testing specimens, where the thickness is the flow direction of the moisture, allowed the moisture gradient along this direction to be neglected.

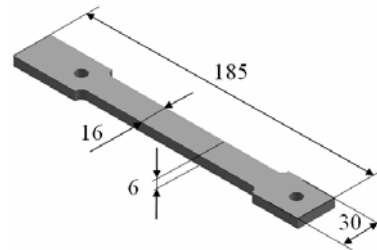


FIGURE 2. Final shape and dimensions (mm) of the tested specimen

Drying simulation at laboratory scale

The equipment used to dry and maintain the air parameters is a new state-of-the-art PGC 0.85 m³ Test Chamber equipped with a SmartPad™ user interface that can allow to control the dry-bulb temperature ($\pm 0.2^\circ\text{C}$) and relative humidity ($\pm 1/2\%$) in a programmable way. The conditioning chamber has a Plexiglas door with three irises which allows inside access without interfering with the experimental conditions.

Four specimens having approximately the same annual rings were subjected to different restraints: zero restraint (free shrinkage), 10% UTS (Ultimate tensile stress), 20% UTS and total restraint (Fig. 3). The free-of-transducers specimen was weighted at different time intervals to determine the moisture change.

The transducers and the load cell were calibrated at room temperature before use and the test temperature influence over the initial calibration was taken into account. The voltage supplied by the transducers was recorded in a computer through a data acquisition system and processed with lab software (Labtech). An initial offset value for each transducer is subtracted from each reading and thus the reading values represent the difference between two consecutive positions.

Experimental design

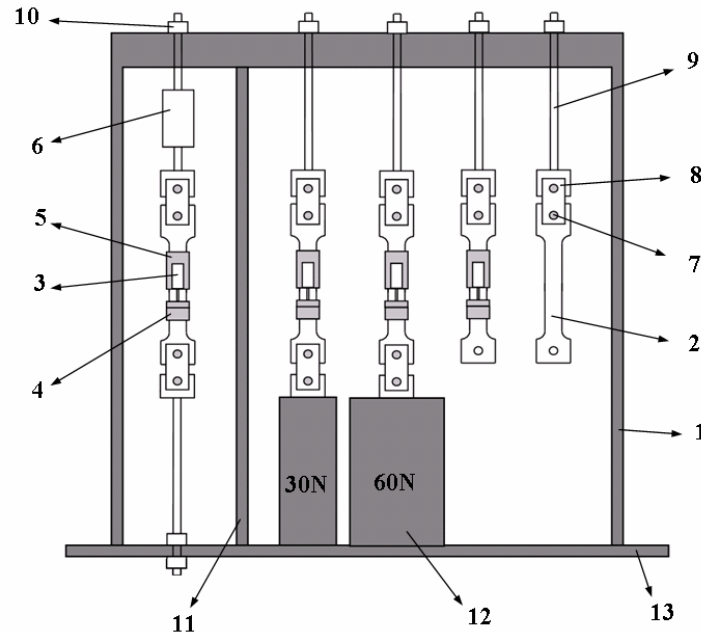


FIGURE 3. Experimental test frame: 1 – rigid steel frame; 2 – free wood specimen; 3 – sprig return linear motion position sensor; 4 – L-shape reference holder; 5 – upper sensor holder; 6 – load cell; 7 – steel rod; 8 – aluminum plate; 9 – threaded rod; 10 – nut; 11 – additional stud; 12 – restraining weight; 13 – frame sole.

Data recording

The deformations were determined during drying by using a pair of LMP (Linear Motion Position) sensors located on the middle part of the sample (Fig. 4). The transducers are fixed on both sides of the specimens and the average value was computed in order to remove bending effects. These sensors can withstand temperatures up to 130°C and each unit consists of a 5kΩ variable resistor over which 1.5V is applied. The upper sensor holder is equipped with two spherical tacks and a conical tack which can penetrate wood surface. The connecting screws between the plates were equipped with springs to maintain the contact between the tacks and wood during the shrinkage process (Fig. 4). A lower L-shape aluminum profile having a similar wood – holder connection system was used as a reference for the sensor extendible rod. The totally restraint sample has a load cell attached on the upper part consisting on 4 strain gauges connected in Wheatstone bridge configuration.

All the samples were conditioned to full saturation; a few measurements after the cutting and storing process proved the existence of a high moisture gradient inside the samples – the middle part had an average with 30% more than the ends. Some of the moisture content is lost during the experiment setup but this value could be quantified and subtracted for modeling purposes.

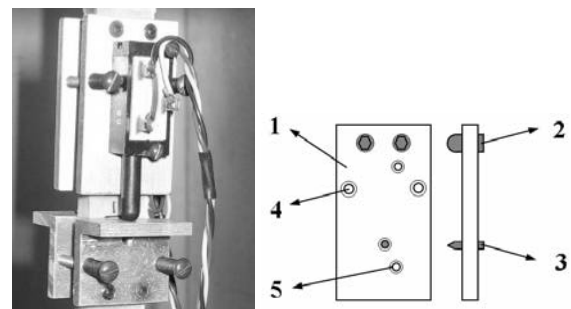


FIGURE 4. Upper sensor holder: 1 – aluminum body; 2 – spherical threaded tack; 3 – sharp threaded tack; 4 – threaded hole for connecting screws; 5 – threaded hole for sensor fixture.

The connection between wood and the restraining system was done using steel rods and aluminum plates. The tensile forces determined by the restraining weights lead to compression in the outer part of the restrained specimen holes. A compression load applied

perpendicular to grain produces stress that deforms the wood cells perpendicular to their length. After the hollow cell cavities are collapsed, wood is quite strong because no void space exists. Wood is usually more than two times stronger in compression than tension perpendicular to grain and this feature allowed assuming that ultimate strength in tension will determine the break point of the specimen. The clamping system has little influence on the partly-restrained specimens, respectively the shrinkage starting time will be delayed and at the beginning the wood will compress in the outer part of the fixing holes before building enough force to lift the weights. For the totally restrained specimen this represented a relaxation way and in order to quantify its effect, two strain transducers were added to this specimens. Therefore, the term “totally restrained” was replaced with the maximum recorded value by the load cell during the drying process.

After the specimens reached the equilibrium moisture content the dead-loads were removed and the elastic, visco-elastic and plastic deformations were recorded. This experimental design allowed a realistic simulation since the stress was induced approximately when wood reached the fiber saturation point.

RESULTS AND DISCUSSION

The strain was calculated by dividing the values given by the sensors (dL , in mm) to the initial distance between the conic tacks ($L = 25.4$ mm):

$$\varepsilon = \frac{dL}{L} \cdot 100 [\%] \quad (2)$$

The results for radial direction at 40°C and 10% target moisture content are illustrated in figures 5 to 9.

The curves show an interesting characteristic (Fig. 5), namely, the restrained specimens swelled with values between 0.17% when restrained by 30N, to 0.59% when restrained by 114N and not only for this particular experiment, but for all. The slow relaxation close to the surface, where the transducers are fixed, might be a combination between the restraining level and temperature in a relation when the higher the temperature and the restraining level, the higher the relaxation. The swelling continued until the surface started to shrink too and enough force was built up for the specimen to start lifting the weights. The positive tensile force value, indicated by the load cell during the swelling process suggests an uneven moisture distribution along the length, with the ends starting to shrink earlier than the middle part of the specimen. For the totally restrained specimen the final shrinkage value is also proportional to the relaxation produced by the

compression.

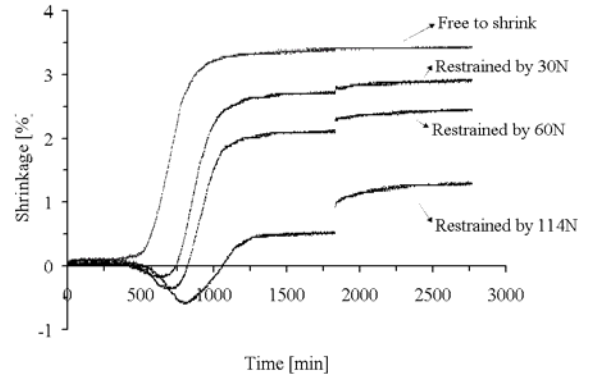


FIGURE 5. Shrinkage strain curves for radial specimens targeting 10% moisture content at 40°C

The shrinkage force diagram illustrated in figure 6 shows a continuous tensile force developed in the specimen during the drying period with some relaxation occurring after the end of drying (~3%).

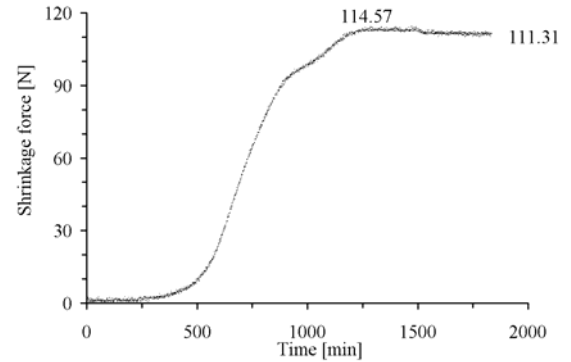


FIGURE 6. Shrinkage force curve for the restrained specimen

The shrinkage percentage for the restrained specimens was calculated as a ratio between the strain developed in the restrained specimen (ε_r^s), divided by the free-to-shrink specimen (ε_f^s) one:

$$Shrinkage = \frac{\varepsilon_r^s}{\varepsilon_f^s} \cdot 100 [\%] \quad (3)$$

The elastic strain was calculated as the difference between the values recorded at the end of the drying process and one minute later after load release. The value was converted in percentage by dividing it to the maximum possible shrinkage (ε_f^s). Similarly, the visco-elastic percentage was calculated as the ratio between the visco-elastic strain and the maximum possible shrinkage (ε_f^s). The “set” or plastic deformation was the unrecoverable strain resulted as a

consequence of creep and mechano-sorptive strain (Fig. 7).

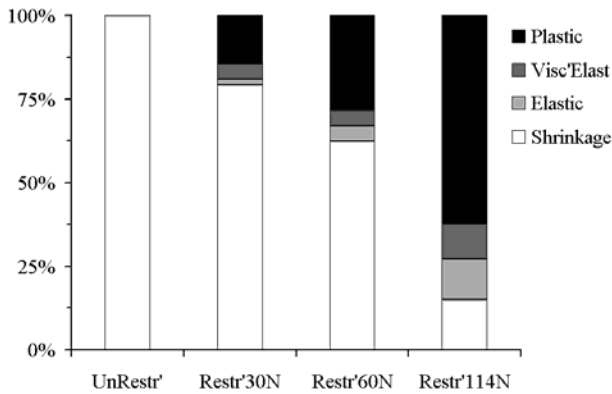


FIGURE 7. Strain components due to restrained drying conditions

Figure 8 illustrates the shrinkage force – final shrinkage strain diagram for different types of restraint, Preliminary experiments suggesting a linear tendency between the restraining level and final shrinkage.

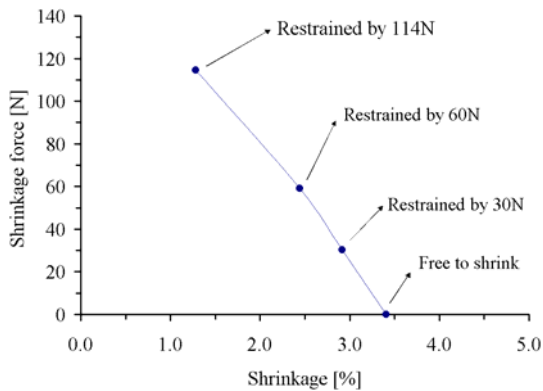


FIGURE 8. Stress - shrinkage curve for different restraining levels

The moisture content curve (Fig. 9) could be determined by dividing the weight of the free specimen, at different intervals of time, to the oven-dry weight. The small thickness of the tested specimens allowed matching the moisture measured results with time by using a surface moisture equation (Crank 1975):

$$M = M_{\infty} + (M_i - M_{\infty}) \cdot e^{-\alpha \cdot t^{\beta}} \quad (4)$$

where M_{∞} represents the moisture content quantity after infinite time, M_i is the initial moisture content and α , β are regression coefficients.

This nonlinear model showed high R^2 coefficients and the assumptions regarding the error term (normality and equal variance) were met.

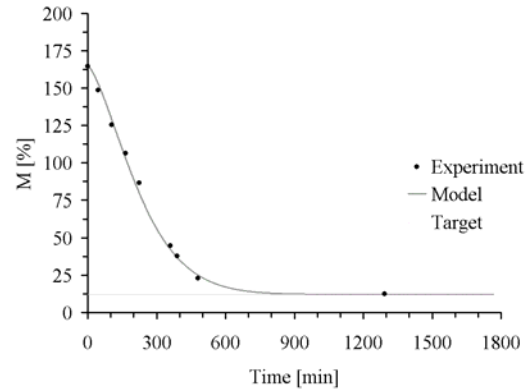


FIGURE 9. Moisture curve for 40C and 56% relative humidity

An increase in temperature reduced considerably the shrinkage force in the restrained specimen in a relationship where the higher the temperature the lower the shrinkage force which is in good agreement with polymer relaxation at higher temperatures (Fig. 10).

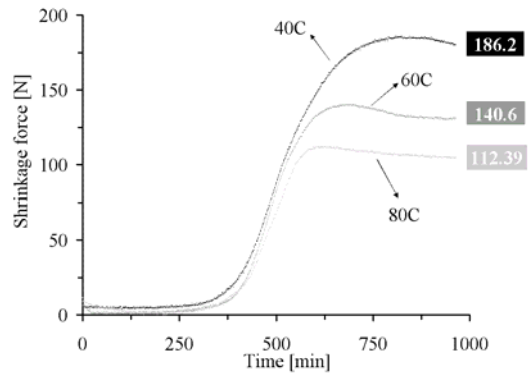


FIGURE 10. Shrinkage force curves for tangential specimens targeting 10% moisture content at different temperatures (40, 60 and 80°C)

This difference is even larger for higher target moisture contents (Fig. 11).

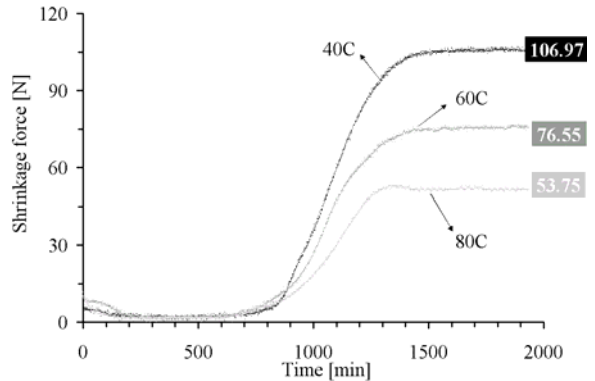


FIGURE 11. Shrinkage force curves for tangential specimens targeting 15% moisture content at different temperatures (40, 60 and 80°C)

CONCLUSIONS

In the light of this preliminary investigation, the following conclusions can be drawn:

1. The experimental design simulates well the stress induced by the core to the shell of drying wood at different restraint levels;
2. The elastic and visco-elastic components of the restrained shrinkage strain can be successfully separated;
3. The set developed in the restrained specimens might be used as an indicator of the restraining level during the drying process.

The next phase of this work will be to measure the restraining level developed by full-size specimens using LMP sensors located around the tested specimen.

ACKNOWLEDGEMENTS

The authors would like to acknowledge the financial support by Natural Sciences and Engineering Research Council of Canada (NSERC).

REFERENCES

- Armstrong, L. D.; Kingston, R. S. T. 1962: The effect of moisture content changes on the deformation of wood under stress. *Aust. J. Appl. Sci.* 13 (4): 257-276.
- Crank, J. 1975. *The mathematics of diffusion.* Oxford University Press.
- Hisada T. 1986: Creep and set behaviour of wood related to kiln drying. *Bull. For. & For. Prod. Res. Inst.* 335, 31-130.
- Majka, J. 2004: Stress development in dependence of the wood drying rate. *Electronic Journal of Polish Agricultural Universities, Wood Technology, Volume 7, Issue 1.*
- Pearson, H.; Evans, R. 2005: Wood quality assessment for stress modeling project. *Wood processing, Issue no. 36, July 2005 Newsletter.*
- Ranta-Maunus A. 1992: Determination of drying stresses in wood when shrinkage is prevented: Test method and modeling. *Proceedings of the 3rd IUFRO International Wood Drying Conference, 1992, Viena, 139-144.*
- Svensson, S. 1995: Shrinkage and shrinkage force in wood under kiln drying conditions. *Holzforschung* 49, 363-368.
- Svensson, S. 1997: *Internal Stresses in Wood Caused by Climatic Variation.* PhD thesis, Lund Institute of Technology Sweden.
- Wu, Q. 1993: *Rheological behavior of Douglas-fir as related to the process of drying.* PhD thesis, Oregon State University.